Bioorganic & Medicinal Chemistry Letters 23 (2013) 4567–4570

Contents lists available at SciVerse ScienceDirect

Bioorganic & Medicinal Chemistry Letters

journal homepage: www.elsevier.com/locate/bmcl

# Synthesis and *in vitro* cellular uptake of $^{11}$C-labeled 5-aminolevulinic acid derivative to estimate the induced cellular accumulation of protoporphyrin IX

Chie Suzuki [a,b], Koichi Kato [c,d,*], Atsushi B. Tsuji [a], Tatsuya Kikuchi [d], Ming-Rong Zhang [d], Yasushi Arano [b], Tsuneo Saga [a]

[a] Diagnostic Imaging Group, Molecular Imaging Center, National Institute of Radiological Sciences, 4-9-1 Anagawa, Inage-ku, Chiba 263-8555, Japan
[b] Department of Molecular Imaging and Radiotherapy, Graduate School of Pharmaceutical Sciences, Chiba University, 1-8-1 Inohana, Chuo-ku, Chiba 260-8675, Japan
[c] Department of Integrative Brain Imaging, National Center of Neurology and Psychiatry, 4-1-1 Ogawahigashi-cho, Kodaira, Tokyo 187-5551, Japan
[d] Molecular Probe Group, Molecular Imaging Center, National Institute of Radiological Sciences, 4-9-1 Anagawa, Inage-ku, Chiba 263-8555, Japan

ARTICLE INFO

*Article history:*
Received 10 May 2013
Revised 7 June 2013
Accepted 11 June 2013
Available online 20 June 2013

*Keywords:*
5-Aminolevulinic acid (ALA)
Photodynamic therapy (PDT)
Sonodynamic therapy (SDT)
Positron emission tomography (PET)
Radiosynthesis

ABSTRACT

Protoporphyrin IX (PpIX) accumulation induced by exogenous 5-aminolevulinic acid (ALA) in tumors affects the therapeutic efficacy of ALA-based photodynamic and sonodynamic therapies. To develop a new imaging probe to estimate the ALA-induced PpIX accumulation, $^{11}$C-labeled ALA analog (**4**), an ALA-dehydratase inhibitor, was radiosynthesized via $^{11}$C-methylation of a Schiff-base-activated precursor in the presence of tetrabutylammonium fluoride, followed by the hydrolysis of ester and imine groups. The cellular uptake of **4** linearly increased with time and was inhibited by ALA and other transporter competitors. Monitoring analog **4** with positron emission tomography might be useful to estimate the ALA-induced PpIX accumulation in tumors.



Photodynamic therapy (PDT)[1] and sonodynamic therapy (SDT)[2] using aminolevulinic acid (ALA)-induced protoporphyrin IX (PpIX) accumulation are promising therapeutic strategies for cancers. ALA is a natural precursor of heme biosynthesis[3] and is photodynamically inert in normal tissues, resulting in low toxicity. PpIX is an intermediate of heme biosynthesis and has both photo- and sono-sensitivities. In tumor tissues, highly selective accumulation of PpIX is induced by exogenous administration of ALA because of low activity of the enzyme that catalyzes the inactivation of PpIX in tumor cells.[4] Highly accumulated PpIX shows cytotoxicity, which is regulated by photo- or sono-irradiation. In clinical studies focusing on ALA-PDT, objective responses were achieved in several cancerous diseases such as nonmelanoma skin[1] and bladder cancers.[5]

Despite the promising results obtained with ALA-PDT, several studies showed that there were apparent differences in the accumulation of ALA-induced PpIX among tumors.[6,7] The differential PpIX accumulation in tumor cells would constitute a key factor affecting the therapeutic efficacy of ALA-based PDT/SDT.[8,9] Therefore, the assessment of ALA-induced PpIX accumulation in tumors can play a significant role in the prediction of the therapeutic effects. Although fluorescence imaging of PpIX can quantify the accumulation of PpIX directly,[10] poor penetration of light hampers its application for deeply seated tumors. On the other hand, positron emission tomography (PET) is an attractive candidate for noninvasive imaging to estimate the PpIX accumulation in tumor irrespective of its location. PET is a noninvasive imaging technology using high-penetrating gamma rays; it enables functional and quantitative assessments of several biologic processes such as transport and metabolism.[11,12] PpIX accumulation is modulated by the influx of ALA via transporters[8,13] and the activity of PpIX synthesis enzymes.[4,14] Therefore, the quantitative PET imaging of ALA influx and/or metabolism of PpIX in tumors could give us helpful information to select patients who could potentially benefit from ALA-based PDT/SDT.

Carbon-11 emits a positron, has a short half-life of 20.4 min and is widely used as a radionuclide for PET chemistry. Although the first choice PET tracer for the above-mentioned purpose would be $^{11}$C-labeled ALA, unfortunately, there are no synthesis pathways to produce $^{11}$C-labeled ALA using [$^{11}$C]$O_2$ or [$^{11}$C]$H_4$ within a short time, which is mandatory because of the short half-life of carbon-11. Therefore, we designed 5-amino-4-oxo-[6-$^{11}$C]hexanoic acid ([$^{11}$C]MALA, **4**) by incorporating a $^{11}$C-methyl group into the position 5 of ALA as a novel PET tracer. Analog **4** is expected to display a similar distribution in the body and incorporation into cells

* Corresponding author. Tel.: +81 42 346 2206; fax: +81 42 346 2229.
*E-mail address:* katok@ncnp.go.jp (K. Kato).

0960-894X/$ - see front matter © 2013 Elsevier Ltd. All rights reserved.
http://dx.doi.org/10.1016/j.bmcl.2013.06.025

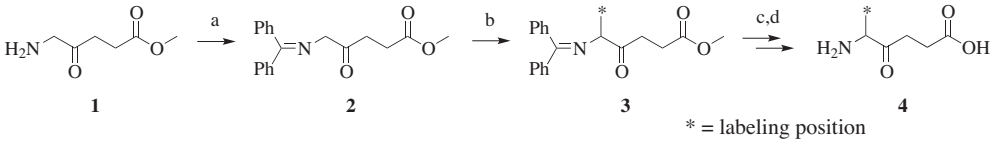


**Scheme 1.** Synthesis of [$^{11}$C]MALA. Reagents: (a) benzophenone imine, dichloromethane; (b) [$^{11}$C]methyl iodide, TBAF, DMSO; (c) NaOH, $H_2O$; (d) HCl, $H_2O$.

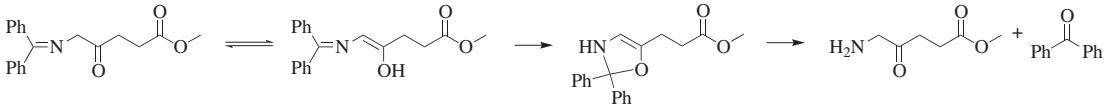

**Scheme 2.** Possible mechanism of the decomposition of **2**.

because of its structural similarity to ALA. In addition, MALA is an inhibitor of 5-aminolevulinate dehydratase (ALAD) through covalent binding to form a carbinolamine intermediate with the catalytic center of ALAD ($K_i$ = 0.2 M).[15] ALAD catalyzes the first step of ALA metabolism to PpIX and is reported to play a major and rate-determining role in regulating PpIX synthesis.[16] After incorporation into tumor cells, **4** is expected to be intracellularly retained depending on the ALAD expression level. Therefore, **4** uptake and/or intracellular retention are candidate predictive factors to estimate the accumulation of ALA-induced PpIX in tumor cells. Herein, we describe the synthesis of **4** and its *in vitro* evaluation in cancer cells.

Schiff-base-activated α-amino acids[17] and peptides[18] are useful precursors for α-alkylation because the enhanced acidity of their α-protons facilitates alkylation reactions with alkyl halides. Various natural and unnatural amino acids and peptides have been synthesized from Schiff base precursors in organic synthesis.[17,18] Concerning $^{11}$C-labeling reactions, we previously reported the synthesis of $^{11}$C-labeled aminoisobutyric acid ([$^{11}$C]AIB) via $^{11}$C-methylation of Schiff-base-activated alanine derivatives by tetrabutylammonium fluoride using [$^{11}$C]methyl iodide ([$^{11}$C]$H_3$I), which is available as a frequently used methylating agent in PET chemistry, in dimethyl sulfoxide (DMSO).[19] The radiochemical yield of [$^{11}$C]AIB was high, and a reproducible synthesis method was established. This experience prompted us to synthesize [$^{11}$C]MALA via $^{11}$C-methylation of a Schiff-base-activated ALA analog (Scheme 1).

For the synthesis of $^{11}$C-labeling precursor **2**, methyl 5-aminolevulinate hydrochloride (**1**) was reacted with one equivalent of benzophenone imine in dichloromethane for 24 h at room temperature (rt). According to thin layer chromatography (TLC) analysis, the spots of **1** and benzophenone imine disappeared, and only one spot corresponding to **2** was newly observed at the end of the reaction, suggesting that the reaction proceeded completely. However, during the purification steps by chromatography on $SiO_2$, **2** decomposed into **1** and benzophenone rapidly. Furthermore, purified **2** decomposed within one day, although many Schiff base derivatives of amino acid esters were reported to be stable.[17,18] The instability of **2** is attributable to the acidity of the protons at position 5. In general, the α-proton of a ketone has higher acidity compared with that of esters, and the increased acidity of **2** could promote keto–enol tautomerization. In fact, proton–deuterium exchange at position 5 was observed when recording a $^1$H NMR spectrum in $CD_3OD$. The hydroxy group of the enol might react with the carbonyl carbon of the imine to produce a five-membered ring intermediate (Scheme 2). The five-membered ring intermediate is then rapidly hydrolyzed to produce **1** and benzophenone.

If unpurified **2** is subjected to the $^{11}$C-methylation reaction, **1**, benzophenone imine, and benzophenone (the decomposition product) will be contained in the labeling precursor. Among these compounds, **2** should be the most reactive against [$^{11}$C]$H_3$I. Therefore, the purification step was skipped and unpurified **2** was used that, in the following experiments, was synthesized just before $^{11}$C-methylation. Moreover, the reaction conditions to prepare precursor **2** was modified; the molar ratio of **1** to benzophenone imine was changed to 2:1 to promote the imination reaction. A shorter reaction time would avoid the decomposition of **2** during the preparation. As a result, according to TLC analysis, benzophenone iminedisappeared within 1 h. Unreacted **1** and $NH_4Cl$, a byproduct of imination, were insoluble and could be removed by filtration. The filtrate was concentrated, and the crude products were immediately used for subsequent $^{11}$C-methylation.

Unpurified **2** dissolved in DMSO was subjected to $^{11}$C-methylion with [$^{11}$C]$H_3$I (18.5–74.0 MBq). The radiochemical identity of $^{11}$C-labeled **3** was verified by comparing its high-performance liquid chromatography (HPLC) profiles with the corresponding unlabeled compound. The reaction efficiency was evaluated from radiochemical conversion (RCC), which was calculated from the radiochromatogram after decay correction. The amount of tetrabutylammonium fluoride (TBAF) was examined to optimize the RCC of [$^{11}$C]$H_3$I to **3**. Similarly, the influence of the timing of TBAF addition was investigated by two distinct reaction approaches: **2** and TBAF were mixed 10 min before the addition of [$^{11}$C]$H_3$I (method A) and TBAF was added to a mixture of **2** and [$^{11}$C]$H_3$I (method B). As shown in Table 1, method B yielded **3** with markedly higher RCCs compared with method A. With regard to the amount of TBAF, 1.0–1.5 μmol of TBAF was required to obtain high RCCs (entries 4 and 5). However, the use of excess amount of TBAF yielded **3** with a lower RCC (entry 6).

In method A, **2** is reacted with [$^{11}$C]$H_3$I following the formation of an anion. On the other hand, in method B, **2** is $^{11}$C-methylated immediately after the anion formation. In both cases, the solution turned yellow immediately after the addition of TBAF to **2**, suggesting fast anion formation. The fast formation of the anion and/or its instability in the presence of TBAF could underlie the higher RCC of $^{11}$C-methylation by method B compared with method A. [$^{11}$C]Methyl iodide (retention time: 4 min) and unknown peaks (retention time: 2–3 min) were observed when **2** was treated with 10 μmol of TBAF by method B (entry 6). The unknown peaks were also observed in the chromatogram of the mixture of [$^{11}$C]$H_3$I and TBAF. Therefore, the formation of several byproducts caused by an excess of TBAF would hamper the desired $^{11}$C-methylation in entry 6.

The following steps were successive alkaline and acid hydrolyses of $^{11}$C-methylated product **3**, and the alkaline hydrolysis conditions of the ester group were explored. The reaction efficiency of ester hydrolysis by NaOH was evaluated after inducing acid hydrolysis of imine to give **4** by the addition of two equivalents of an aqueous solution of HCl to NaOH. Because product **4** was a small

**Table 1**
[$^{11}$C]Methylation of **2**

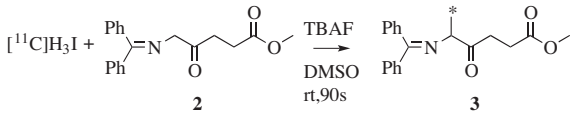


**2** **3**

| Entry | $n$[a] | TBAF (μmol) | Method | RCC[b] (%) |
|---|---|---|---|---|
| 1 | 1 | 1.0 | A | 2.8 |
| 2 | 1 | 10 | A | 5.1 |
| 3 | 3 | 0.5 | B | 40.8 ± 18.4 |
| 4 | 6 | 1.0 | B | 75.6 ± 6.4 |
| 5 | 1 | 1.5 | B | 75.6 |
| 6 | 2 | 10 | B | 35.3, 45.2 |

[a] $n$ means number of repetitions.
[b] Radiochemical conversion (RCC) was calculated by a radiochromatogram obtained using analytical RP-HPLC following decay correction.

**Table 2**
Hydrolysis of **3**

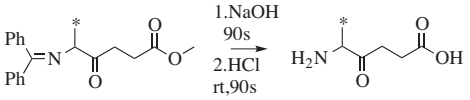


**3** **4**

| Entry | $n$[a] | NaOH (mol/L) | Temperature (°C) | RCC[b] (%) |
|---|---|---|---|---|
| 1 | 1 | 6 | 100 | 0 |
| 2 | 2 | 1 | 100 | 4.7, 7.7 |
| 3 | 2 | 1 | 40 | 11.5, 21.5 |
| 4 | 2 | 0.1 | 100 | 8.7, 44.3 |
| 5 | 1 | 0.1 | 40 | 51.4 |
| 6 | 6 | 0.1 | rt | 51.9 ± 8.2 |
| 7 | 1 | 0.05 | 40 | 7.5 |

[a] $n$ means number of repetitions.
[b] RCC was calculated by a radiochromatogram obtained using analytical HILIC–HPLC following decay correction.

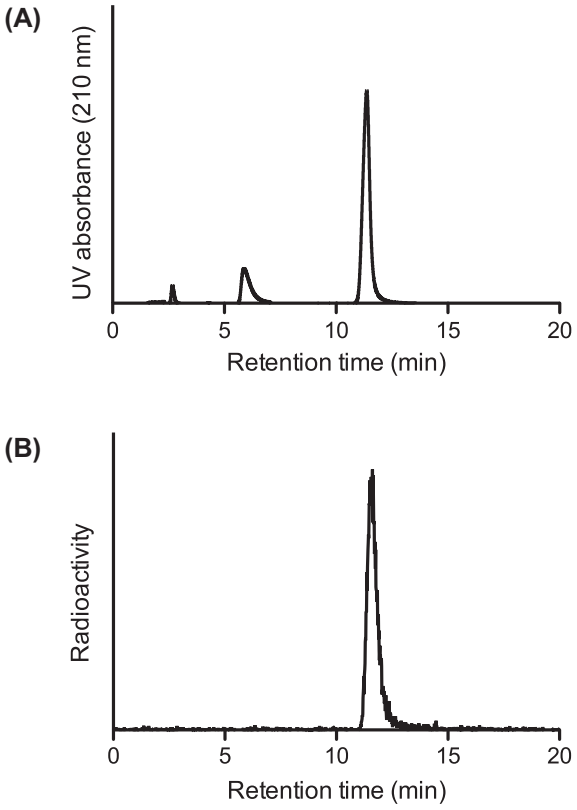


**Figure 1.** HPLC profiles of MALA. (A) UV absorbance (210 nm) of unlabeled MALA. (B) Radioactivity levels of [$^{11}$C]MALA.

polar molecule, a hydrophilic interaction chromatography (HILIC) column was used for HPLC analysis. As shown in Table 2, **4** was obtained with high RCC under mild conditions (entries 5 and 6), whereas under high NaOH concentration or high reaction temperature conditions, byproducts more hydrophobic than **4** (entries 1–4) were detected. Because some amount of imine moiety of **3** was hydrolyzed during alkaline hydrolysis, **4** and its methyl ester were present in the reaction mixture. These two compounds were unstable in basic conditions because of the formation of pyrazine compounds[20] and cyclization via intramolecular aminolysis of δ-amino ester,[21] respectively. The above-mentioned hydrophobic byproducts might be formed via these side reactions.

After the optimization of the $^{11}$C-methylation and hydrolyses reactions, remote-controlled synthesis of **4** was conducted to enhance the starting radioactivity. Each step of the synthesis was performed under the above-mentioned conditions, and desired product **4** was purified by semipreparative HPLC. In this synthesis, the final pH of the reaction mixture containing **4** was around 5, which enabled direct injection into the HPLC system without adjusting the pH. The total time to synthesize **4** from the end of bombardment (EOB) to formulation, including [$^{11}$C]$H_3$I production and purification, was approximately 35 min. The final amount of radioactivity was 0.43–1.85 GBq and radiochemical yield was 4.4 ± 1.7% (decay uncorrected, referred to [$^{11}$C]carbon dioxide, $n$ = 10) when the synthesis was started from 11.8 to 29.6 GBq of [$^{11}$C]carbon dioxide at EOB. After purification, a single peak was observed (Fig. 1B) at the same retention time of the corresponding unlabeled compound (Fig. 1A), and the radiochemical purity (RCP) was 97.5 ± 1.9% ($n$ = 6). The peak of UV absorption at 210 nm of ALA was not observed in the chromatogram of purified **4**. The amount of radioactivity of **4** was sufficient to conduct *in vitro* and *in vivo* studies.

The shelf-life stability study of **4** (206.0 MBq/mL) in an aqueous solution at rt showed that RCP was more than 95% after 60 min. When **4** was incubated with murine serum at 37 °C, the serum protein binding fraction was 2.7 ± 0.3% ($n$ = 3), as determined by an ultrafiltration method. The percentage of the fraction of intact **4** after 60 min of incubation in serum was 97.4 ± 0.7% ($n$ = 3), as determined by HPLC. These findings indicate that **4** possesses the stability sufficient for running PET studies and low serum protein binding useful for imaging at early post-injection intervals.

Under the present synthetic procedure, **4** is obtained as a racemic mixture at position 5. Although chiral biomolecules generally show enantiospecific biological properties such as substrate recognition of transporters or enzymes,[22] *in vitro* studies were preliminarily conducted to evaluate whether **4** was worth further research. Because there are no studies conducted on MALA uptake transporter(s) to date, we investigated whether **4** and ALA share similar transport systems. ALA is transported into cells via oligopeptide transporters 1 and 2 (PEPT1/2)[23] and/or beta transporters.[24] Cellular uptake study was therefore conducted using the AsPC-1 cell line, which highly expresses PEPT1/2.[25] In inhibition study, glycylsarcosine (Gly-Sar, a substrate of PEPT) and γ-aminobutyric acid (GABA, a substrate of beta transporters) were used as an inhibitor of the corresponding transporters in addition to ALA. As shown in Figure 2A, **4** showed linearly increasing uptake over 30 min. When cells and **4** were incubated in the presence or absence of ALA, Gly-Sar, or GABA, all substrates inhibited **4** uptake in a dose-dependent manner in the range of 0.1 to 1 mM (Fig. 2B). The inhibitory effect reached a plateau at more than 1 mM of Gly-Sar and GABA, whereas ALA exhibited a complete

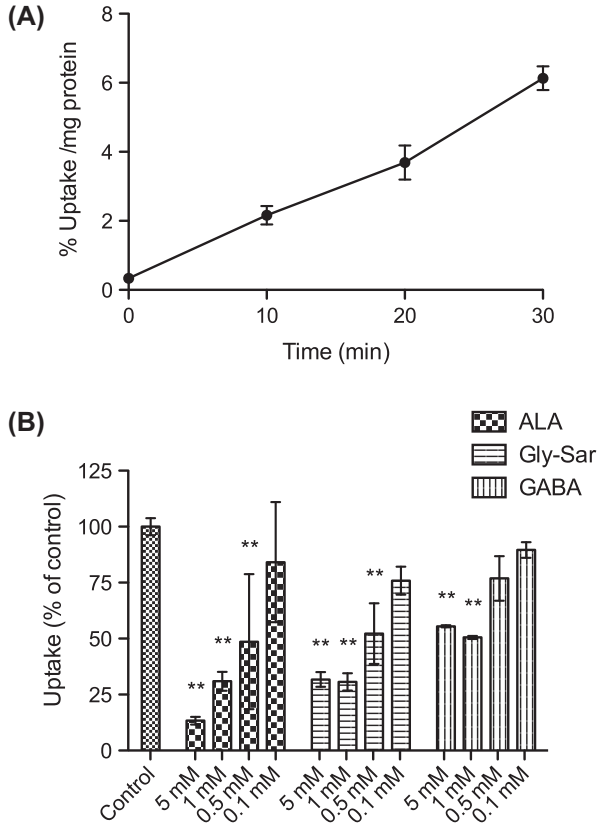


**Figure 2.** Cellular uptake of [$^{11}$C]MALA in AsPC-1 cells. (A) Time-dependent uptake of [$^{11}$C]MALA at 37 °C. The values are expressed as the percentage of administered radioactivity at different times. (B) Effect of the putative inhibitors of [$^{11}$C]MALA. The cells were incubated with [$^{11}$C]MALA for 10 min at 37 °C. The values are expressed as the percentage of uptake relative to the control uptake without ALA and inhibitors. Each point and column represents the mean ± SD of three monolayers. $^{**}P$ <0.01 compared with the control analyzed by ANOVA with Dunnett's multiple comparison test.

dose-dependent and marked inhibition at the high concentration. These results suggest that **4** would be transported by both PEPT and beta transporters, sharing similar transport systems with ALA. Therefore, **4** would constitute a potential candidate for PET imaging of ALA influx and/or metabolism for PpIX in tumors.

In conclusion, we successfully synthesized **4**, a $^{11}$C-labeled ALA derivative, with sufficient radioactivity for imaging and high radiochemical purity using one-pot procedure by the remote-controlled system. The stability of **4** was adequate for *in vivo* imaging with PET. The cellular uptake of the racemic mixture of **4** was mediated by transporters at least partially similar to those of ALA. Because MALA was reported to bind to ALAD, the pharmacokinetics of **4** could partly reflect ALA metabolism. We anticipate that [$^{11}$C]MALA-PET has the potential to evaluate the amount of ALA-induced PpIX, a predictive factor of the therapeutic effects of ALA-based PDT and SDT.

## Acknowledgments

We would like to thank the staff of the Cyclotron Operation and Radiochemistry sections for the production of the radioisotope, the technical support of the remote-controlled synthesis, and the identification of compounds by mass spectral analysis. This work was supported in part by KAKENHI23510289, 24591803, and 25861136.

## Supplementary data

Supplementary data associated with this article can be found, in the online version, at http://dx.doi.org/10.1016/j.bmcl.2013.06.025.

## References and notes

1. Peng, Q.; Warloe, T.; Berg, K.; Moan, J.; Kongshaug, M.; Giercksky, K. E.; Nesland, J. M. *Cancer* **1997**, *79*, 2282.
2. Ohmura, T.; Fukushima, T.; Shibaguchi, H.; Yoshizawa, S.; Inoue, T.; Kuroki, M.; Sasaki, K.; Umemura, S. *Anticancer Res.* **2011**, *31*, 2527.
3. Franken, A. C.; Lokman, B. C.; Ram, A. F.; Punt, P. J.; van den Hondel, C. A.; de Weert, S. *Appl. Microbiol. Biotechnol.* **2011**, *91*, 447.
4. Ohgari, Y.; Nakayasu, Y.; Kitajima, S.; Sawamoto, M.; Mori, H.; Shimokawa, O.; Matsui, H.; Taketani, S. *Biochem. Pharmacol.* **2005**, *71*, 42.
5. Kriegmair, M.; Baumgartner, R.; Lumper, W.; Waidelich, R.; Hofstetter, A. *Br. J. Urol.* **1996**, *77*, 667.
6. Gibbs, S. L.; Chen, B.; O'Hara, J. A.; Hoopes, P. J.; Hasan, T.; Pogue, B. W. *Photochem. Photobiol.* **2006**, *82*, 1334.
7. Widhalm, G.; Wolfsberger, S.; Minchev, G.; Woehrer, A.; Krssak, M.; Czech, T.; Prayer, D.; Asenbaum, S.; Hainfellner, J. A.; Knosp, E. *Cancer* **2010**, *116*, 1545.
8. Hagiya, Y.; Endo, Y.; Yonemura, Y.; Takahashi, K.; Ishizuka, M.; Abe, F.; Tanaka, T.; Okura, I.; Nakajima, M.; Ishikawa, T.; Ogura, S. *Photodiagn. Photodyn. Ther.* **2012**, *9*, 204.
9. Kinoshita, M.; Hynynen, K. *Radiat. Res.* **2006**, *165*, 299.
10. Valdes, P. A.; Leblond, F.; Kim, A.; Harris, B. T.; Wilson, B. C.; Fan, X.; Tosteson, T. D.; Hartov, A.; Ji, S.; Erkmen, K.; Simmons, N. E.; Paulsen, K. D.; Roberts, D. W. *J. Neurosurg.* **2011**, *115*, 11.
11. Haberkorn, U.; Markert, A.; Mier, W.; Askoxylakis, V.; Altmann, A. *Oncogene* **2011**, *30*, 4141.
12. Strauss, L. G.; Conti, P. S. *J. Nucl. Med.* **1991**, *32*, 623.
13. Nakanishi, T.; Tamai, I. *J. Pharm. Sci.* **2011**, *100*, 3731.
14. Takahashi, K.; Ikeda, N.; Nonoguchi, N.; Kajimoto, Y.; Miyatake, S.; Hagiya, Y.; Ogura, S.; Nakagawa, H.; Ishikawa, T.; Kuroiwa, T. *Neuro. Oncol.* **2011**, *13*, 1234.
15. Erskine, P. T.; Newbold, R.; Brindley, A. A.; Wood, S. P.; Shoolingin-Jordan, P. M.; Warren, M. J.; Cooper, J. B. *J. Mol. Biol.* **2001**, *312*, 133.
16. Feuerstein, T.; Schauder, A.; Malik, Z. *Photochem. Photobiol. Sci.* **2009**, *8*, 1461.
17. O'Donnell, M. J.; Bennett, W. D.; Bruder, W. A.; Jacobsen, W. N.; Knuth, K.; Leclef, B.; Polt, R. L.; Bordwell, F. G.; Mrozack, S. R.; Cripe, T. A. *J. Am. Chem. Soc.* **1988**, *110*, 8520.
18. Ooi, T.; Tayama, E.; Maruoka, K. *Angew. Chem., Int. Ed.* **2003**, *42*, 579.
19. Kato, K.; Tsuji, A. B.; Saga, T.; Zhang, M. R. *Bioorg. Med. Chem. Lett.* **2011**, *21*, 2437.
20. Gadmar, O. B.; Moan, J.; Scheie, E.; Ma, L. W.; Peng, Q. *J. Photochem. Photobiol. B* **2002**, *67*, 187.
21. Taylor, P. J. M.; Bull, S. D.; Andrews, P. C. *Synlett* **2006**, 1347.
22. Qu, W.; Zha, Z.; Ploessl, K.; Lieberman, B. P.; Zhu, L.; Wise, D. R.; Thompson, C. B.; Kung, H. F. *J. Am. Chem. Soc.* **2009**, *133*, 1122.
23. Novotny, A.; Xiang, J.; Stummer, W.; Teuscher, N. S.; Smith, D. E.; Keep, R. F. *J. Neurochem.* **2000**, *75*, 321.
24. Bermudez Moretti, M.; Correa Garcia, S.; Perotti, C.; Batlle, A.; Casas, A. *Br. J. Cancer* **2002**, *87*, 471.
25. Gonzalez, D. E.; Covitz, K. M.; Sadee, W.; Mrsny, R. J. *Cancer Res.* **1998**, *58*, 519.